4036–4048 *Nucleic Acids Research, 2013, Vol. 41, No. 7* *Published online 26 February 2013*
doi:10.1093/nar/gkt100

Coactivators enable glucocorticoid receptor recruitment to fine-tune estrogen receptor transcriptional responses

Michael J. Bolt[1], Fabio Stossi[1], Justin Y. Newberg[1], Arturo Orjalo[2], Hans E. Johansson[2] and Michael A. Mancini[1,*]

[1]Department of Molecular and Cellular Biology, Baylor College of Medicine, Houston, TX 77030, USA and [2]Biosearch Technologies Inc., Novato, CA 94949, USA

Received October 25, 2012; Revised January 11, 2013; Accepted January 28, 2013

ABSTRACT

Nuclear receptors (NRs) are central regulators of pathophysiological processes; however, how their responses intertwine is still not fully understood. The aim of this study was to determine whether and how steroid NRs can influence each other's activity under co-agonist treatment. We used a unique system consisting of a multicopy integration of an estrogen receptor responsive unit that allows direct visualization and quantification of estrogen receptor alpha (ERα) DNA binding, co-regulator recruitment and transcriptional readout. We find that ERα DNA loading is required for other type I nuclear receptors to be co-recruited after dual agonist treatment. We focused on ERα/glucocorticoid receptor interplay and demonstrated that it requires steroid receptor coactivators (SRC-2, SRC-3) and the mediator component MED14. We then validated this cooperative interplay on endogenous target genes in breast cancer cells. Taken together, this work highlights another layer of mechanistic complexity through which NRs cross-talk with each other on chromatin under multiple hormonal stimuli.

INTRODUCTION

Estrogen receptor alpha (ERα) is a ligand-activated transcription factor that plays important pathophysiological roles in multiple tissues, including mammary gland, uterus (1,2) and bone (3,4). ERα is a member of the nuclear receptor (NR) superfamily characterized by modular structural domains (A–F) (5) that include transactivation AF1 (A/B) and AF2 (E/F) regions, DNA-binding (C) and hormone-binding (E/F) functions. Ligand-bound ERα dimerizes and dynamically binds to estrogen response elements (EREs) throughout the genome; subsequently, ERα can serve as a platform for the recruitment of histone-modifying enzymes and transcriptional co-regulators that modulate chromatin structure and RNA polymerase II action, impinging directly on target gene regulation. Co-regulator proteins, such as p160s (SRC-1, -2 and -3) (6) and mediator (7) families, have been shown to greatly affect ERα-mediated transcription through direct interactions primarily with the AF2 region.

Recent studies highlighted a varied and intricate web of different transcription factors that are responsible for finely tuned ERα-mediated transcriptional output. For example, ERα regulates the expression of other transcription factors, such as GATA3, FOXA1, MYC, PGR, FOS and PITX1 (8–11), which can then feedback on ERα signaling by working as pioneer factors, by marking the genomic landscape, by changing ERα expression and/or by directly modulating transcriptional output of secondary target genes, thus creating a fine tuned phenotypic response to hormone. An additional layer of complexity resides in the cross-talk between ERα and other transcription factors when these are simultaneously activated by their own agonistic stimuli. This phenomenon, despite its physiological relevance, is less well studied. The best example of this in the NR field has been the analysis of the interplay between ERα and retinoic acid receptors in breast cancer cells, which showed both cooperative (12) and antagonistic (13) effects on ERα-mediated transcription after combination of estrogenic and retinoid stimuli. Other systems have shown similar interplay between NRs and transcription factors (14,15).

Of the 48 NRs (16), seven comprise type I steroid receptors [e.g. androgen receptor (AR), ERα, ERβ, progesterone receptors (PR-A and PR-B), MR and glucocorticoid receptor (GR)], and this subfamily is particularly important in a wide range of normal

*To whom correspondence should be addressed. Tel: +1 713 798 8952; Fax: +1 713 790 0545; Email: mancini@bcm.edu
Present address:
Michael A. Mancini, Department of Molecular and Cellular Biology, Baylor College of Medicine, Houston, TX 77030, USA.

physiological and pathological conditions (17,18). In the current study, we aimed to investigate the molecular cross-talk between type I NRs by using a unique tool developed in our laboratory, the GFP-ERα:PRL-HeLa array cell line (19–22). The GFP-ERα:PRL-HeLa model consists of multicopy integration of an estrogen responsive transcriptional reporter gene derived from the regulatory region (promoter and enhancer) of the rat prolactin (PRL) gene [(23); e.g. PRL array] and also stably expresses GFP-ERα (green fluorescent protein-tagged) at levels comparable with MCF-7 breast cancer cells. The PRL array model allows for direct quantitative visualization of multiple transcriptional mechanisms via multiplex fluorescence microscopy, and it is readily amenable to the type of high-throughput analysis required to study complex systems level issues in gene regulation.

After an initial immunofluorescence analysis of all type I NRs (minus MR), we decided to focus on the cross-talk between ERα and GR. It is increasingly clear that understanding the mechanisms underlying this cross-talk has great potential in studying multiple disease states, including inflammatory diseases and cancer. For example, in breast cancer, ERα, which is expressed in ca. 70% of tumors (24), is currently the primary target for therapeutic intervention. Additionally, glucocorticoids have been used for many years in the treatment of breast cancer to fight inflammatory processes and side effects of chemotherapy (25) with a wide range of effects observed *in vivo* (26,27) and *in vitro*.

Enabled by quantitative analysis of GFP-ERα:PRL-HeLa cells using automated multiparametric image analysis, we show here that other type I NRs, but not other members of the superfamily, are recruited to the ERE-rich array only when ERα is present and under dual ligand treatment (e.g. in the presence of agonists for both receptors). Deletion mutant analyses reveal that co-recruitment of GR to the PRL array is dependent on the co-regulator interaction domain of ERα (e.g. helix-12 in the ligand-binding domain). Through a small co-regulator siRNA survey, we identified SRC-2, SRC-3 and MED14 as essential ERα-binding partners required for GR recruitment. Importantly, fluorescent *in situ* hybridization (FISH) studies indicate that co-recruitment of GR has a negative impact on ERα-mediated transcriptional stimulation. Next, we extended our analysis in breast cancer cells and found examples of genes and enhancers where the ERα/GR cross-talk occurs and has various gene-specific outcomes (e.g. cooperation and antagonism). Taken together, this study reveals unappreciated functional chromatin interplay between ERα and GR that depends on co-regulator recruitment and results in both cooperative and antagonistic transcriptional regulation as part of the fine tuning of hormonal responses.

MATERIALS AND METHODS

Cell culture and immunolabeling

GFP-ERα:HeLa-PRL cells were maintained in Dulbecco's modified Eagle's medium containing 10% fetal bovine serum (FBS) (Gemini Bioproducts), 1 nM Tam (Sigma), 200 μg/ml of hygromycin, 0.8 μg/ml of blastocidin, sodium pyruvate and L-glutamine. Cells were plated for 48 h in 5% stripped-dialyzed FBS, phenol red free-Dulbecco's modified Eagle's medium before treatment on standard 12-mm glass coverslips or 384-well optical glass (Greiner) or plastic (Aurora; siRNA experiments) plates.

For immunolabeling, cells were fixed in 4% formaldehyde in PEM buffer (80 mM potassium PIPES, pH 6.8, 5 mM EGTA and 2 mM $MgCl_2$), quenched with 0.1 M ammonium chloride and permeabilized with 0.5% Triton X-100. Cells were incubated at room temperature in blotto (5% milk in 1× TBS–Tween 20) for 1 h, and then specific antibodies were added overnight at 4°C. The antibodies used were anti-GR (GeneTex GTX101120), RNA polymerase II (ABCAM ab5408), PPARγ (ABCAM ab52270), ERα (Millipore 04-820), Ser5-phospho RNA polymerase II (ABCAM ab5401), MED14 (Bethyl A301-044 A), SRC-2 (BD Transduction Labs # 610985) and SRC-3 (BD Transduction Labs # 611105). After washes, the cells were incubated at room temperature for 1 h with Alexa Fluor 647 goat anti-rabbit IgG or Alexa Fluor 647 goat anti-mouse IgG (Molecular probes). This was followed by two PEM washes and another fixation and quench step before DAPI (1 μg/ml) staining. Coverslips were mounted on slides using SlowFade Gold (Invitrogen S36937).

Fluorescence *in situ* hybridization

Cells were fixed in 4% paraformaldehyde in RNase-free phosphate-buffered saline for 15 min and then permeabilized with 70% ethanol in RNase-free water at 4°C for 1 h. Cells were washed in 1 ml of wash buffer (2× SSC (Ambion) and 10% formamide) followed by hybridization in hybridization buffer (1 g of dextran sulfate, 1 ml of 20× SSC buffer, 1 ml of formamide and 8 ml of nuclease-free water) with RNA probes (dsRED2 Stellaris™ probes, Biosearch Technologies Inc.) for 4 h at 37°C followed by one wash in wash buffer for 30 min at 37°C and then DAPI stain for 10 min at 37°C. Finally, cells were washed in 2× SCC buffer followed by mounting using SlowFade Gold.

Transfections, plasmids and RNAi experiments

GFP-ERα, GFP-ERα (amino acids 1–534), GFP-ERα (amino acids 1–554) and GFP-GR plasmids were described previously (22). mCherry-GR was created by removing the GR from GFP-GR, using BamHI and BsrGI restriction sites and inserting it into the mCherry-C2 vector. Cells were reverse transfected using Lipofectamine 2000 reagent (Invitrogen 11668-500) for 4–6 h. For RNAi experiments, we used Lipofectamine RNAiMax (Invitrogen 13778-150) along with 8 nM siRNA. PRL-HeLa cells were transfected for 72 h.

Imaging and quantification

Automated imaging was carried out using the Cell Lab IC-100 Image Cytometer (IC100, Beckman Coulter) at room temperature using CytoShop 2.0. Image acquisition was performed with a Nikon S Fluor 40×/0.90 NA objective. Z-stacks were imaged at 1 μM intervals at 1 × 1

binning. Nuclear array segmentation and signal quantization were performed using PipelinePilot image analysis software as previously described (20). Briefly, maximum intensity projections were created for the GFP-ERα and antibody channels followed by background subtraction to all images. Nuclei were defined by DAPI signal and masks created by applying adaptive thresholding followed by marker-based watershed. Array segmentation was based on thresholding of the GFP-ERα image. Aggregated cells, mitotic cells and apoptotic cells were removed using filters based on nuclear size, nuclear shape and nuclear intensity.

Deconvolved images were taken using a DeltaVision Core Image Restoration Microscope (Applied Precision) at room temperature. Z-stacks were imaged at 0.2 μM intervals with a 60×/1.42 NA Plan Achromat objective and a charge couple device camera (CoolSnap HQ2; Photometrics). These images were also taken at 1 × 1 binning.

Quantitative reverse transcriptase–polymerase chain reaction and chromatin immunoprecipitation

MCF-7 cells were treated with 10 nM E2, 100 nM Dex or E2 + Dex for 45 min before the chromatin immunoprecipitation (ChIP) procedures. Cells were fixed with 1% formaldehyde for 10 min at room temperature, lysed in RIPA (Sigma-Aldrich) buffer, sonicated and then the soluble fraction pre-cleared for 1 h with protein A/G agarose beads. Pull-downs were then performed using the HC-20 anti-ERα antibody (Santa Cruz) and Pierce Rbt anti-GR (Thermo Scientific). After the IP, protein A/G agarose beads were added and washed sequentially with high salt, low salt and TE buffers. DNA was then eluted and analyzed by quantitative real-time polymerase chain reaction (PCR) using specific primers for the ER-binding sites closest to selected ER-regulated genes.

Total RNA was isolated using Trizol® as per manufacturer's instructions. One microgram of total RNA was reverse transcribed in a total volume of 20 μl using 200 U reverse transcriptase, 50 pmol random hexamers and 1 mM dNTPs (New England Biolabs, Beverly, MA, USA). The resulting cDNA was analyzed with real-time PCR. Each real-time PCR reaction consisted of 6 μl of diluted reverse transcribed product, 1× SYBR Green PCR Master Mix (Applied Biosystems, Foster City, CA, USA) and 50 nM of forward and reverse primers. Reactions were carried out in an Applied Biosystems StepOne Plus for 40 cycles (95°C for 15 s, 60°C for 1 min). The fold change in expression was calculated using the ΔΔ Ct comparative threshold cycle method, with the ribosomal protein 36B4 mRNA as an internal control.

Statistical analysis and software

Data presented were acquired from a minimum of three independent experiments performed on different days with different passages of cells. *P*-value was determined using student's *t*-test for single comparisons or one-way ANOVA for independent samples and a Tukey HSD post-hoc test for comparisons across multiple samples.

The data for the heat map in Figure 5A were generated using Cluster 3.0 using hierarchical clustering with a centroid linkage method (28) and then visualized using Java Treeview (29).

RESULTS

Type I nuclear receptors load onto the PRL array only after ERα recruitment

We have previously generated and characterized the PRL-HeLa array cell line stably expressing GFP-ERα (GFP-ERα:PRL-HeLa) as a model to visually study and inspect the mechanisms linked to ERα mediated transcriptional regulation by high-throughput fluorescence microscopy and high-content analysis (19–22,30,31). To expand our knowledge of the interplay between multiple transcription factors at the integrated transcription locus, we performed bioinformatic analysis of the promoter/enhancer elements that comprise the PRL array to determine the full complexity of additional transcription factor-binding sites. Using web-based motif analysis software (e.g. Alibaba and JASPAR), we identified several putative transcription factor-binding motifs (CEBP, AP1 and GATA) in the PRL promoter/enhancer, including a steroid/hormone response element (HRE/SRE) located close to the ERE/Pit1 synergy element (Figure 1A for diagram).

With our longstanding interest in the molecular biology of type I NRs coupled with the recent findings from the various laboratories on transcription factor interplay (12–15), we asked whether there were endocrine conditions where the HREs/SREs within the PRL array could be occupied by combinations of type I NRs. Although all GFP-ERα:PRL-HeLa cells exhibit nuclear ERα, the multicopy PRL locus becomes visibly 'loaded' only when ligand treated; when it is grown in media containing stripped/dialyzed serum, virtually no nuclei exhibit a visible array. To this end, we transfected the parental PRL array-containing HeLa cells (PRL-HeLa, which are ERα negative) with GFP-tagged versions of five type I NRs e.g. AR, PR-A, PR-B and GR) either alone (not shown) or in co-transfection with mCherry-ERα and treated them for 30 min with 100 nM dexamethasone (for GR), 10 nM dihydroxytestosterone (DHT) (for AR) or 10 nM R5020 (for PR-A and PR-B). Our results are summarized in Figure 1B–E and reveal that under NR agonist alone conditions (except for E2, see later in the text) in stripped/dialyzed serum-containing media, GFP-AR (Figure 1B), GFP-GR (Figure 1C), GFP-PRB (Figure 1D) and GFP-PRA (Supplementary Figure S1B) all failed to load onto the PRL array. Further, as expected, the non-ER type I NRs did not load the PRL array with E2 treatment; in contrast, 17β-estradiol (E2) treatment readily induced array formation in all ERα-expressing cells (middle column Figure 1B–E). However, combining E2 treatment with any of the agonists for type I NRs (i.e. dexamethasone, DHT and R5020) induced loading of both ERα and type I NRs as highlighted by the arrows (third column Figure 1B–E) and is indicative of an ERα 'cooperative loading' mechanism. As

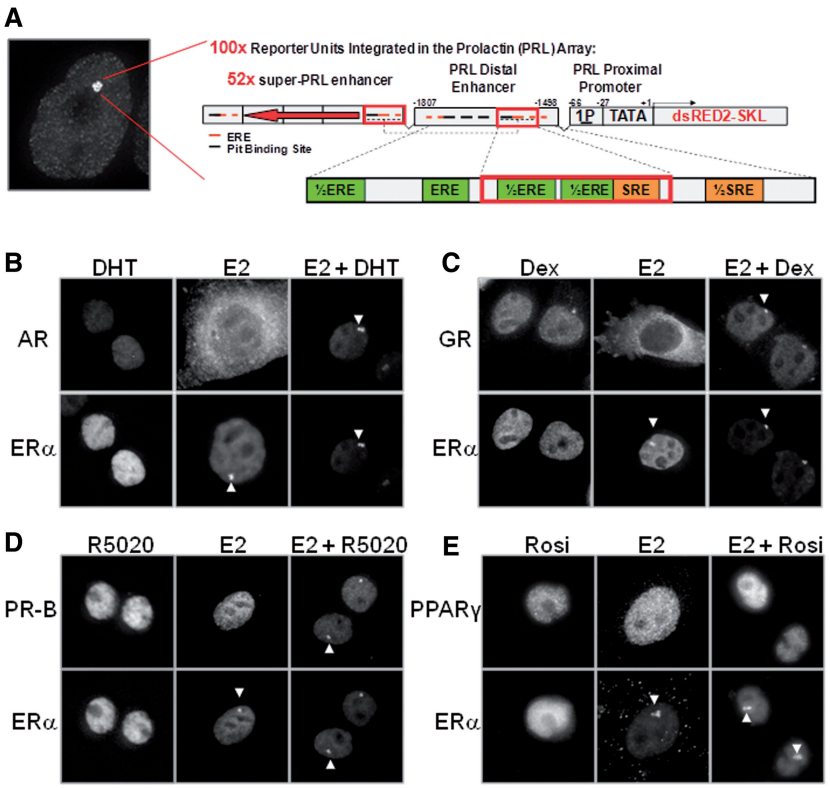

Figure 1. Type I NRs localize to the PRL array only under dual ligand conditions. (**A**) Schematic representation of the PRL array that was stably integrated into the PRL-HeLa array cell line along with GFP-ERα. (**B**) Images of transfected ERα (bottom row) and AR (top row) in PRL HeLa cells treated with 10 nM DHT, 10 nM E2 or E2 + DHT. (**C**) Images of transfected ERα (bottom row) and GR (top row) in PRL HeLa cells treated with 100 nM Dex, 10 nM E2 or E2 + Dex. (**D**) Images of transfected ERα (bottom row) and PR-B (top row) in PRL HeLa cells treated with 10 nM R5020, 10 nM E2 or E2 + R5020. (**E**). Images of transfected ERα (bottom row) and PPARγ (top row) in PRL-HeLa cells treated with 10 nM Rosi, 10 nM E2 or E2 + Rosi. White arrows indicate the location of NR loading onto the PRL array.

an additional control, we also examined a non-type I NR, PPARγ (Figure 1E), which does not recognize HRE/SRE-binding motifs. Indeed, PPARγ was unable to load onto the PRL array either after treatment with its own agonist (rosiglitazone) alone or in combination with E2 (Figure 1E), suggesting that the 'cooperative loading' observed in Figure 1 does not occur with all NRs.

We were also interested in whether ERβ, which can localize to the PRL array with E2 (31), was able to cause recruitment of the type 1 NRs to the PRL array. To determine whether the cooperative loading was able to occur with ERβ, we transfected GFP-GR and ERβ-mCherry and treated with 10 nM E2 + 100 nM Dex. As seen in Supplementary Figure S1B, GR was able to localize to the PRL array element with ERβ. Because of the relatively low homology between ERα and ERβ N-termini, these data are also suggestive that the N-terminus of ERα may not be important for the cooperative loading.

To determine whether the NRs binding to the PRL array is dependent on DNA binding to the SRE/HRE, we transfected wild-type PR-B or PR-B with a mutated DNA binding domain (DBD), which makes it unable to bind directly to DNA, PR-B DBDmut (32), into PRL-HeLa cells constitutively expressing GFP-ERα and treated them with Veh or 10 nM E2 + 10 nM R5020. Wild-type PR-B was able to colocalize to the PRL array with ERα on dual agonist treatment (Supplementary Figure S1C), whereas the PR-B DBDmut was unable to do so under either condition (Supplementary Figure S1D). These data strongly suggest that localization to the PRL array of the type 1 NRs after treatment with E2 + agonist is dependent on DNA binding to a SRE/HRE sequence.

Loading of endogenous GR onto the PRL array is ERα-dependent and maximal when both receptors are agonist bound

Next, we wanted to confirm that the observed 'cooperative loading' between NRs was not due to overexpression of the partners or the presence of tags (GFP and mCherry). We decided to focus on GR due to its endogenous expression in the PRL-HeLa array cell line, and due to the growing body of literature discussing different modes of cross-talk between glucocorticoids and estrogens (33–35). To assess loading of endogenous GR onto the PRL array, we performed antibody labeling for GR in the GFP-ERα:PRL-HeLa cell line treated with vehicle, 10 nM E2, 100 nM Dex or E2 + Dex for 30 min. As expected, GR translocated into the nucleus (Figure 2A, bottom panels) under Dex or E2 + Dex treatments, but GR loading onto the PRL array was only evident after dual agonist treatment (E2 + Dex; arrows in Figure 2A as

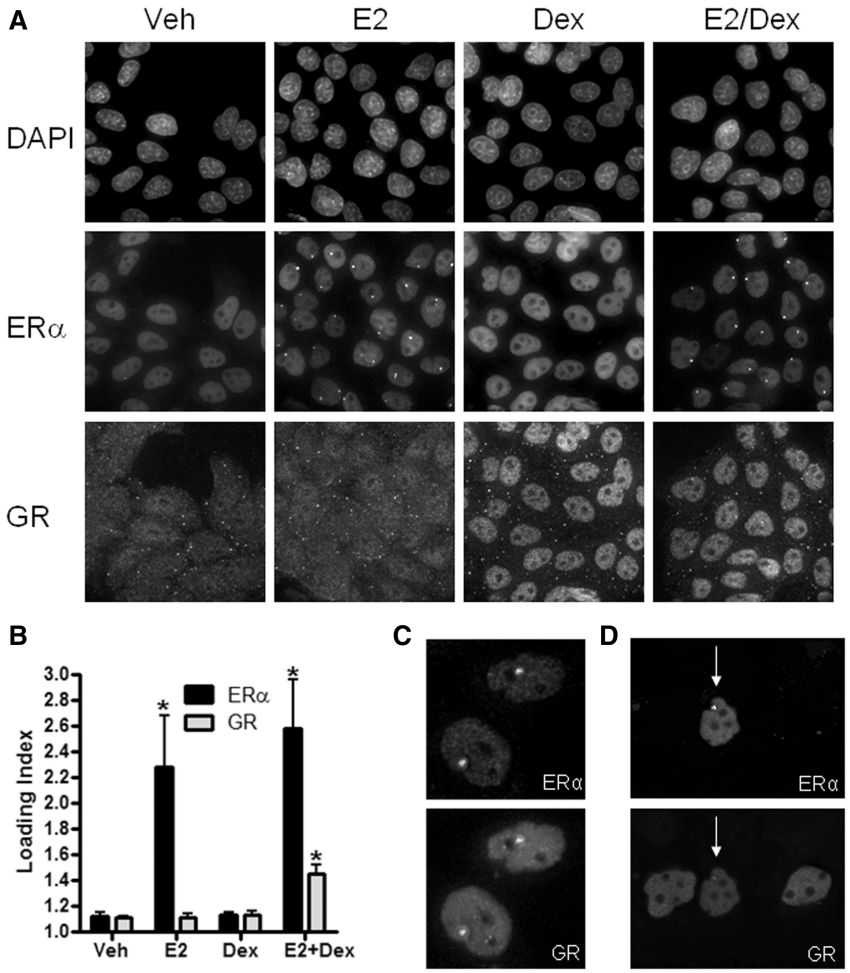

Figure 2. Endogenous GR localizes to the PRL array under dual agonist conditions. (**A**) Representative fields of PRL-HeLa:GFP-ERα cells treated with 5% EtOH (veh), 10 nM E2, 100 nM Dex or 10 nM E2 + 100 nM Dex, showing DAPI, GFP-ERα and GR staining. (**B**) Quantification of ERα and GR loading index (mean intensity of signal at array/mean intensity of signal in the nucleoplasm) using PipelinePilot Image Analysis software. $*P < 0.05$. More than 1000 cells/condition were analyzed. (**C**) ERα and GR were transfected into PRL-HeLa cells treated with E2 + Dex and show localization to the PRL array. (**D**) mCherry-tagged ERα and GFP-tagged GR were transfected into PRL-HeLa cells and treated with E2 + Dex. Only the cell that has both ERα and GR shows GR localization to the PRL array (white arrows).

examples). This was also true when ERβ, instead of ERα, -containing cells were used (Supplementary Figure S1B). We quantified the amount of GR that loaded onto the PRL array (Figure 2B) by using a custom image analysis protocol developed on the Pipeline Pilot Image Analysis platform (PLP; see 'Materials and Methods' section for details). The PLP platform permits us to perform robust analysis of ERα functions by segmenting array and nucleoplasm regions and then quantify, on a cell-by-cell basis, the amount of any labeled factor present at the PRL array. We calculated a loading index for GR and ERα, which is defined as the mean intensity of GR or ERα signal at the array divided by the mean intensity of GR or ERα signal in the nucleoplasm. Using this metric with automated microscopy, we were able to quantify >1000 cells per treatment and observed a significant increase in ERα loading to the PRL array on E2 and E2 + Dex treatments (with no effect of Dex on ERα loading); in contrast, GR loading onto the PRL array was significantly increased only after E2 + Dex treatment (Figure 2B). We also performed time course and hormone dose–response curves and measured ERα and GR loading, and per cent of cells with an array and array size to fully characterize this cooperative interplay (Supplementary Figure S2).

We then wanted to determine whether the loading of GR onto the PRL array was influenced by the GFP-tag fused to ERα. To verify this was not the case, we transfected untagged ERα or mCherry-ERα into parental PRL-HeLa cells and treated them with E2 + Dex to determine whether GR still exhibited cooperative loading. After dual agonist treatments, GR localized onto the array with each version of ERα demonstrating that the cooperative loading is not dependent on the type, presence or location of the fluorescent tag. The immunolabeling images for untagged ERα are shown in Figure 2C. To discern whether GR loading onto the PRL array is ERα-dependent or may be due to other signaling

pathways (e.g. via non-genomic actions or GPR30 activation), we co-transfected PRL-HeLa with GFP-GR and mCherry-ERα and treated them with E2 + Dex for 30 min. Figure 2D shows that GR recruited onto the PRL array only in dual-transfected cells (white arrow). In cells where no ERα expression is evident, GR did not target the PRL array, indicating that cooperative loading is dependent on nuclear ERα loading onto the PRL array.

We next wanted to evaluate whether cooperative loading was dependent on specific classes of ligands (i.e. agonists versus antagonists) for either ERα or GR. To this goal, we first treated the GFP-ERα:PRL-HeLa cells with vehicle, 100 nM Dex or the GR antagonist RU486 (100 nM) in the presence of 10 nM E2 for 30 min (Figure 3A). Although RU486 treatment did cause an increased GR loading onto the PRL array, it was significantly less compared with Dex treatment (33% reduction). Similarly, when we treated with ERα antagonists [10 nM 4-hydroxy-tamoxifen (Tam) or 100 nM Fulvestrant (ICI)] in the presence of 100 nM dexamethasone (Figure 3B), we saw that both Tam and ICI were able to cause recruitment of GR onto the PRL array but at a significantly lower level than E2 + Dex (66% reduction). Representative images are shown in Supplementary Figure S3. Collectively, the data shown in Figure 3A and B suggest that GR loading onto the PRL array is maximal when both receptors are in an agonist conformation.

GR loading onto the PRL array correlates with ERα loading but not array area, GR level or ERα level

High content analysis allows us to mine image data sets with hundreds of features per individual cell. These

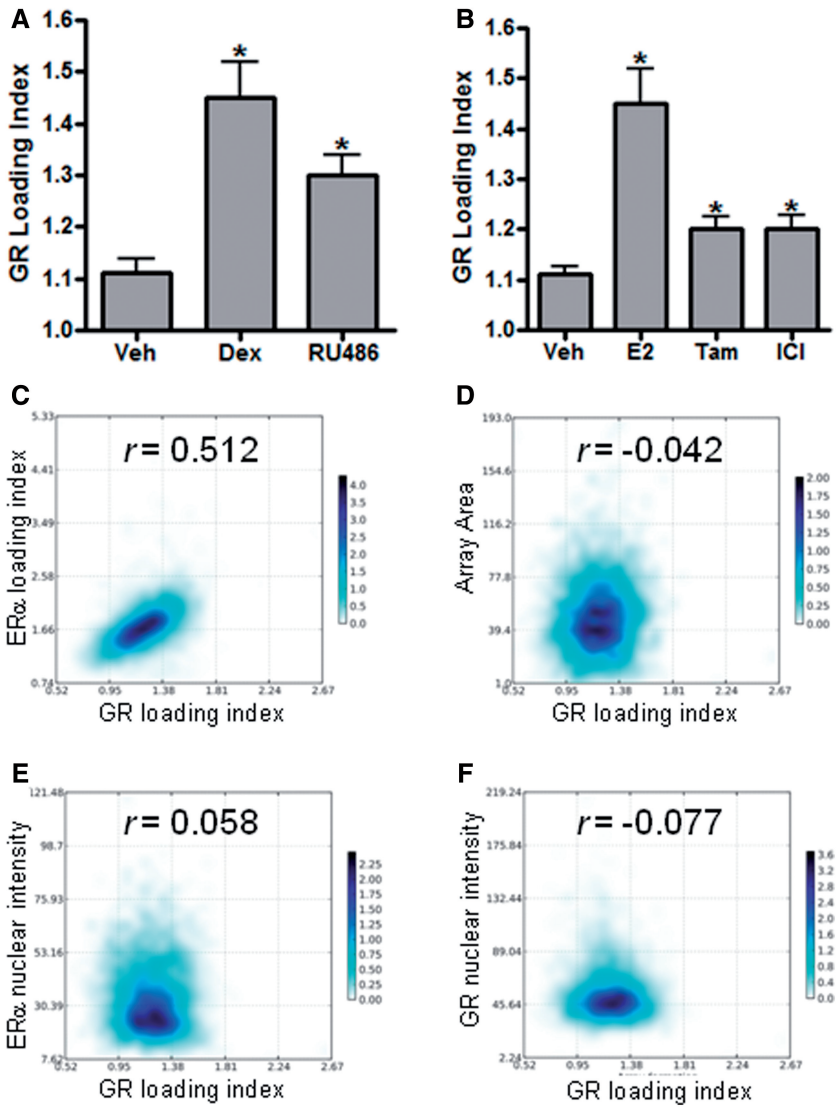

Figure 3. ERα, E2 and Dex are required for maximal GR loading. (**A**) Quantification of GR loading index in the presence of 10 nM E2 with either 5% EtOH (veh), 100 nM Dex or 100 nM RU486. (**B**) Quantification of GR loading index in the presence of 100 nM Dex with vehicle, 10 nM E2, 10 nM Tam or 100 nM ICI. $*P < 0.05$ compared with veh treatment. (**C–F**) Single-cell scatter plot of GR loading index (*x*-axis) with ERα loading index (C), array area (D), ERα nuclear intensity (E) or GR nuclear intensity (F) on the *y*-axis. Values above each plot are correlation coefficients quantified using Pearson's product moment.

features are descriptors of various mechanistic or cytological characteristics of the fluorescent signals being examined; they are linked to protein expression, intracellular and intranuclear localization and so forth. We chose four basic features directly linked to transcriptional regulation, ERα binding to DNA, chromatin remodeling, ERα nuclear protein level and GR nuclear protein level, and we used them to determine whether a correlation exists between this feature set and GR loading onto the PRL array. Figure 3C–F show scatter plots of single cell values for E2 + Dex treatment with the *x*-axis being the GR loading index and *y*-axis corresponding to one of the four chosen features. No statistically significant correlation was observed between GR loading index and array area (Figure 3D), ERα nuclear levels (Figure 3E) or GR nuclear levels (Figure 3F). Conversely, GR loading index did significantly correlate (Pearson's $r = 0.5126$) with ERα loading index (Figure 3C), providing additional evidence that an ERα loaded PRL array is required for GR PRL array occupancy.

GR loading onto the PRL array is dependent on ERα helix-12

To further explore the mechanism(s) through which ERα assists GR recruitment onto the PRL array, we wanted to determine which domain of ERα is required. We transiently co-transfected PRL-HeLa cells with mCherry-GR and GFP-tagged wild-type ERα or mutant ERα vectors that have previously been used in the study for the regulation of ERα (36). We compared wild-type ERα with a helix-12 truncation (amino acids 1–534), which eliminates the interaction domain for the p160 family of co-regulators (e.g. SRC-3) and an F domain truncation (amino acids 1–554) (Figure 4A). Cells were then treated with E2 + Dex for 30 min and immunolabeled with an antibody to RNA polymerase II (Pol II) and GR (Figure 4A), or SRC-3 and GR (Figure 4B). As expected, wild-type ERα was able to recruit GR, Pol II and SRC-3. The F-domain mutant (amino acids 1–554) was also able to recruit GR, Pol II and SRC-3. The mutant ERα lacking helix-12 (amino acids 1–534) was capable of loading onto the PRL array; however, it failed to recruit GR, Pol II or SRC-3. These data indicate that GR recruitment onto the PRL array is mediated through helix-12 and requires an intact ligand-binding domain and, as shown later in the text in detail, may involve other co-regulators (Figure 5).

MED14, SRC-2 and SRC-3 mediate GR loading onto the PRL array

To identify potential co-regulators that mediate GR loading onto the PRL array, we performed a small siRNA survey directed against a panel of well-established modulators of transcription, including the p160 family of co-regulators (SRC-1, -2 and -3), LEO1, DDX3X, MED14 and Sin3B. We also used GR siRNA as positive control and scrambled siRNA as negative control. GFP-ERα:PRL-HeLa cells were transfected with the siRNA panel for 72 h and were then treated for 30 min with 10 nM E2 + 100 nM Dex; after fixation, cells were immunolabeled to localize GR and the more active serine 5-phosphorylated form of RNA polymerase II. We were thus able to perform high-content analysis to determine the effects of each siRNA on nuclear intensity (levels), array intensity (array int) and array loading for ERα, GR and serine 5 phosphorylated Pol II. Figure 5A shows a heat map summarizing the results from the siRNA knockdown analysis. Although most of the genes tested (SRC-1, SRC-2, SRC-3 and so forth) have little effect on PRL array features (SRC-3 siRNA results in a loss of active Pol II at the array, whereas Sin3B has the opposite effect), the three outliers (combination SRC-2/-3, GR and MED14) all cause a significant decrease in GR loading. Light blue indicates reduction, whereas yellow

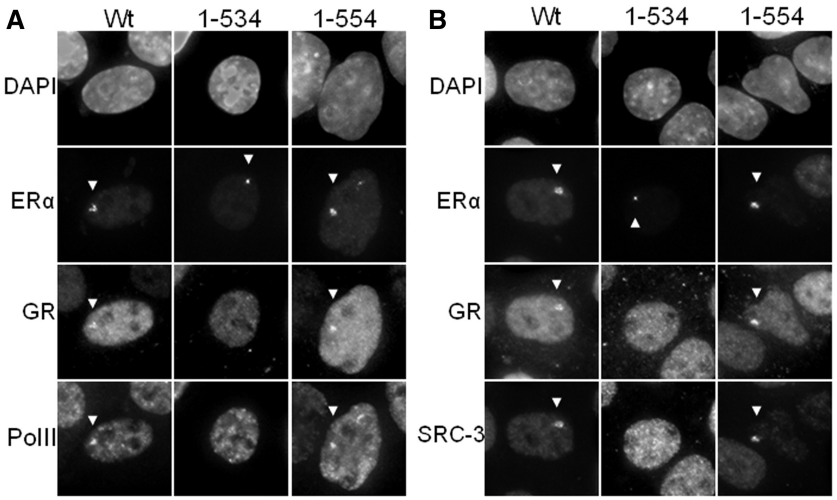

Figure 4. ERα mutants demonstrate importance of ERα helix-12 in GR recruitment. (**A and B**) GFP-tagged ERα mutants (full length, amino acids 1–534 or amino acids 1–554) were transfected along with mCherry-tagged GR into PRL-HeLa cells and treated with E2 + Dex for 30 min. Cells were labeled with antibody targeting RNA polymerase II (A) or SRC-3 (B). White arrows indicate the location of NR, SRC-3 or RNA polymerase II loading onto the PRL array.

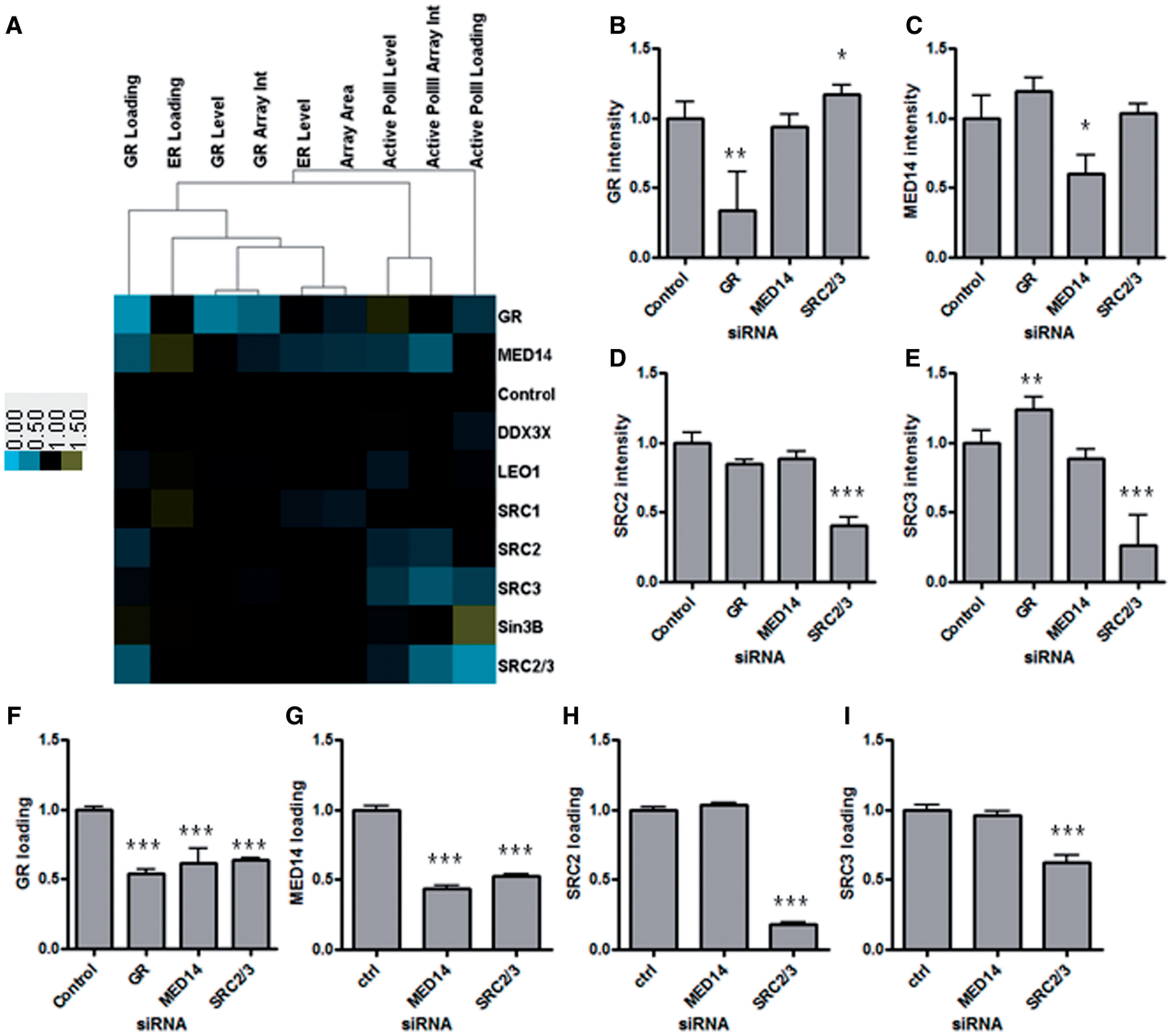

Figure 5. MED14, SRC-2 and SRC-3 mediate the recruitment of GR to the PRL array. (**A**) Heat map showing effects of siRNA knockdown of multiple factors on features of the PRL array system, including GR loading, active RNA polymerase II loading and ER loading. (**B**) Quantification of GR nuclear intensity (normalized to control siRNA) after 72 h siRNA knockdown of GR, MED14 and SRC-2/-3 in HeLa-PRL:GFP-ERα cells treated with 10 nM E2 + 100 nM Dex for 30 min. (**C**) Quantification of MED14 nuclear intensity (normalized to control siRNA). (**D**) Quantification of SRC-2 nuclear intensity (normalized to control siRNA) treated as described earlier in the text. (**E**) Quantification of SRC-3 nuclear intensity (normalized to control siRNA). (**F**) Quantification of GR loading (normalized to control siRNA) after 72 h siRNA knockdown of GR, MED14 or SRC-2/-3 in HeLa-PRL:GFP-ERα cells treated with 10 nM E2 + 100 nM Dex for 30 min. (**G**) Quantification of MED14 loading (normalized to control siRNA) after 72 h siRNA knockdown of MED14, or SRC-2/-3 in HeLa-PRL:GFP-ERα cells treated with 10 nM E2 + 100 nM Dex for 30 min. (**H**) Quantification of SRC-2 loading (normalized to control siRNA) after 72 h siRNA knockdown of MED14, or SRC-2/-3 in HeLa-PRL:GFP-ERα cells treated with 10 nM E2 + 100 nM Dex for 30 min. (**I**) Quantification of SRC-3 loading (normalized to control siRNA) after 72 h siRNA knockdown of MED14, or SRC-2/-3 in HeLa-PRL:GFP-ERα cells treated with 10 nM E2 + 100 nM Dex for 30 min (*$P < 0.05$; **$P < 0.005$; *** $P < 0.0005$).

reflects an increase in each of the nine parameters examined compared with scrambled siRNA (black). As a control, in Figure 5B, we show effective GR knockdown (e.g. reduced GR nuclear intensity and array loading without affecting ER levels or array loading).

We next tested which co-regulator knockdowns specifically impacted GR loading on the PRL array without affecting global GR nuclear levels. High-content analysis of the RNAi survey identified MED14, a subunit of the mediator complex, and to a lesser extent SRC-2, as essential for GR PRL array loading after treatment with both E2 and Dex (Figure 5A). Intriguingly, a combination of SRC-2 and SRC-3 siRNAs produced a greater reduction in GR loading (Figure 5E) compared with single knockdowns of the p160 co-regulators. We validated siRNA knockdown efficacy by immunofluorescence microscopy as shown in Figure 5B–D and Supplementary Figures S4 and S5D. SRC-2, SRC-3 and MED14 are all recruited to the PRL array on both E2 and E2 + Dex conditions with no statistical difference

between the two treatments (Supplementary Figure S5A–C).

To infer the spatial interrelationships between SRCs and MED14 that lead to GR loading, we knocked down GR (Figure 5B), MED14 (Figure 5C) and SRC-2/-3 (Figure 5D–E, respectively) and then quantified the loading of GR (Figure 5F), MED14 (Figure 5G), SRC-2 (Figure 5H) and SRC-3 (Figure 5I). Knockdown of SRC-2/-3 decreased loading of GR and MED14, and, as expected, also SRC-2, and SRC-3, whereas MED14 siRNA only blocked MED14 and GR loading. These data suggest that SRC-2 and SRC-3 are required for MED 14 loading, which is then responsible for GR loading.

GR presence at the PRL array causes reduction in E2-induced reporter gene transcription

To better understand the functional consequences of ERα-GR cross-talk, we sought to directly quantify the effect of E2 + Dex treatment directly on transcriptional output from the PRL array by using RNA FISH directed against the dsRED2 reporter gene mRNA. GFP-ERα:PRL-HeLa cells were treated with vehicle, E2 or E2 + Dex for a time course ranging from 5 min to 24 h, and accumulation of the PRL-regulated dsRED2 reporter gene mRNA was measured by RNA FISH using a highly specific fluorescently labeled probe set (Stellaris^{TM}, Biosearch Technologies). As shown in Figure 6A, the dsRED2 mRNA was rapidly induced by E2 treatment and E2 + Dex treatment alike. Around 6 h after treatment, E2 + Dex treatment resulted in significantly less mRNA than E2 treatment alone, indicating that loading of GR on the PRL array ultimately leads to a transcriptional repressive effect.

Complex ERα/GR interplay on chromatin in MCF-7 breast cancer cells

We next wanted to determine whether ERα/GR cooperative chromatin loading and transcriptional interplay was occurring at any known ERα target genes in an endogenous setting. Using MCF-7 breast cancer cells that had been treated with 5% EtOH, 10 nM E2, 100 nM Dex or E2 + Dex for 24 h, we performed qPCR on two well-characterized ERα target genes, TFF1 (pS2, Figure 6B) and GREB1 (Figure 6D). TFF1 mRNA levels, increased with E2, were reduced with Dex and showed a muted E2 response in the E2 + Dex treatment. We then performed ChIP assays for ERα and GR to determine their recruitment to the TFF1 enhancer after 45 min of treatment (Figure 6C). As expected, ERα recruitment to the TFF1 enhancer was increased by E2 treatment and did not change by addition of Dex. We also show that GR is recruited to the same enhancer under both Dex and E2 + Dex treatments without showing any statistically significant difference. In contrast to TFF1, GREB1 is induced by both E2 and Dex with a synergistic increase in the double treatment. On analysis of ERα ChIP-seq data (37), it is clear that the GREB1 genomic locus is rich in ERα binding sites. By ChIP–PCR analysis, we found two of these ER-binding sites (GREB_732 and GREB_734) that show significant increases in GR binding compared with vehicle (Figure 6E and F, respectively), but only when treated with E2 + Dex, with minimal effects on ERα binding (Figure 6E–F). The effect of Dex alone is likely because of novel GR-binding elements in the GREB1 locus, as indicated by ChIP-seq analysis (K. P. White, personal communication). These data not only recapitulate what we observed in the PRL array model system but also highlight gene- and enhancer-specific effects that can occur in an endogenous setting, which we are continuing to explore.

DISCUSSION

NRs are a key group of transcription factors that regulate gene regulation programs in many diverse tissues where they serve as rheostats that respond to external and hormonal stimuli. The organismic distribution of NRs shows both widespread and tissue-specific expression (38), indicating that extensive interplay between numerous hormones at the same time must occur. Moreover, it is well known that combinatorial expression of NRs in tumors (i.e. breast cancer) is important in determining prognosis and avenues of treatment (39,40). Despite the obvious complexity of multiple NRs functioning simultaneously in any cellular milieu, thus far studies interrogating NR function(s) have been most extensively examining only one hormone at a time; regardless, these highly reductionist approaches have provided early essential insight into NR actions. Notable exceptions include studies comparing GR with PR actions (41,42) or ERα with retinoic acid receptors (12,13); collectively, these efforts showed both competitive and cooperative interactions. To quantitatively explore the functional complexity and interplay of type I NRs with visual tools, we have used an engineered multicopy estrogen responsive transcriptional array system (PRL array) and high-throughput microscopy as an assay platform. The PRL array system affords us with a unique opportunity to visualize by fluorescence microscopy and quantify, on a cell-by-cell basis using high-content analysis, all the major steps involved in ERα-mediated transcriptional activation, including receptor and co-regulator recruitment, histone modifications, chromatin changes and transcriptional output.

After bioinformatics analysis that revealed an additional NR-binding site in the PRL enhancer, we used the PRL array model to explore potential functional interplay between ER and other type I NRs at the chromatin level. Our observations that dual ligand treatments (e.g. E2 + another agonist) are required for ERα to recruit GR (or other type I NRs, but not PPARγ) to the adjacent HRE/SRE are consistent with an assisted loading mechanism similar to recently described by Voss *et al.* (15). However, Voss *et al.* analyzed the cross-talk of two NRs on a single *cis*-element using wild-type GR and an ERα point mutant that alters ERα specificity from ERE to GRE binding. In the current study, we used the PRL model to analyze the interplay between two distinct *cis*-elements (ERE versus HRE/GRE) using two wild-type NRs (ERα and GR).

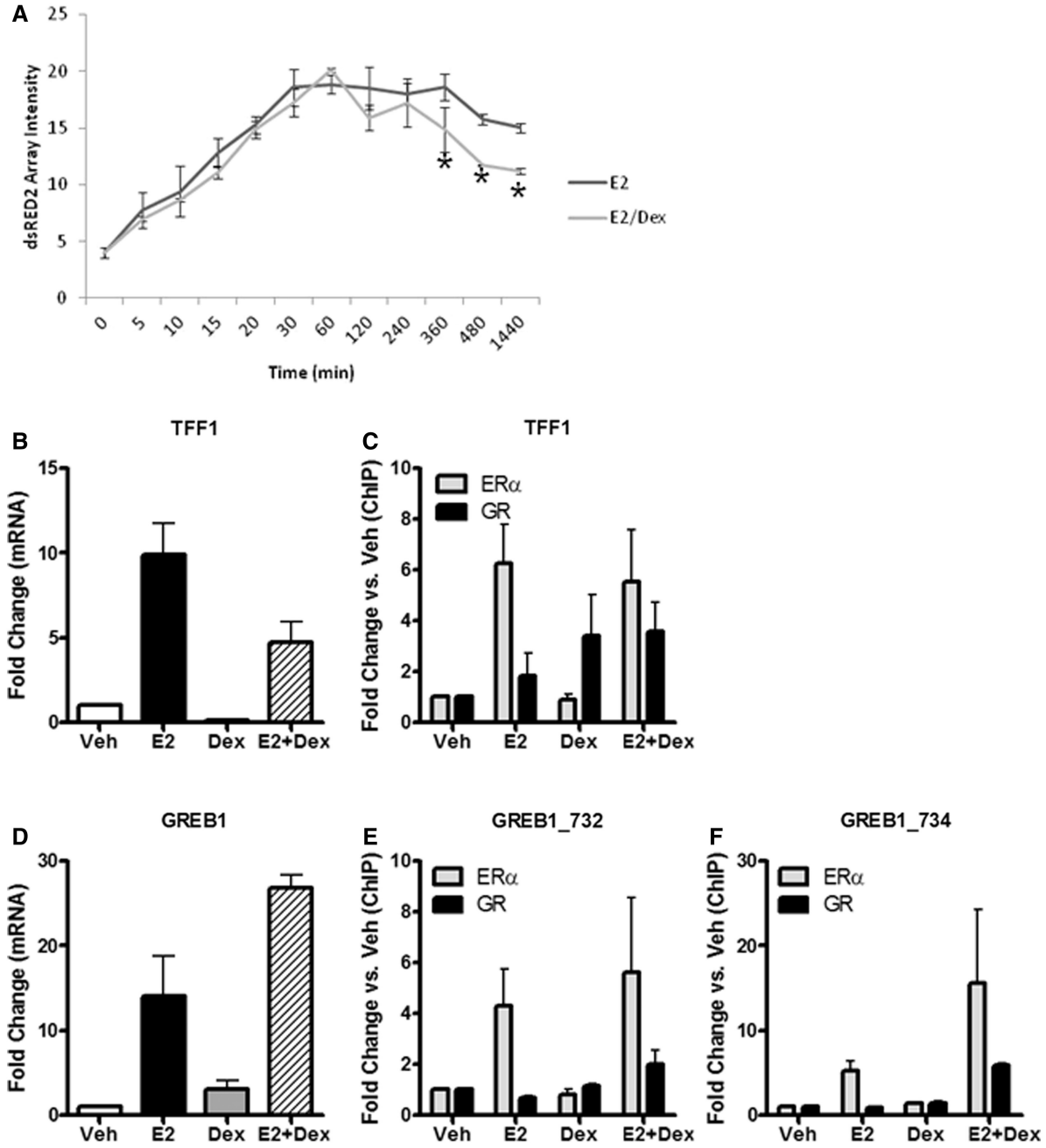

Figure 6. ERα/GR cross-talk effects transcriptional output in PRL array and MCF-7 cell systems. (**A**) Time course of dsRED2 mRNA production at the PRL array when treated with 10 nM E2 or 10 nM E2 + 100 nM Dex and measured by RNA FISH. $*P < 0.05$ versus E2. (**B**) TFF1 mRNA levels were measured by qPCR when treated for 24 h with 5% EtOH (V), 10 nM E2 (E), 100 nM Dex (D) or 10 nM E2 + 100 nM Dex (E + D). (**C**) ChIP assay showing ERα (gray) and GR (black) recruitment to the TFF1 enhancer region after 45 min of treatments mentioned in (B). Data are normalized to vehicle treatment. (**D**) GREB1 mRNA levels were measured by qPCR after 24 h of treatment. (**E** and **F**) ChIP assay showing ERα (gray) and GR (black) recruitment to two enhancer regions (732 and 734, respectively) of the GREB1 genomic locus after 45-min treatments.

We report here our quantitative observations of *de novo* loading of type I NRs onto the PRL array only under dual ligand treatment (i.e. ERα ligand + type I NR ligand). Collectively, these data suggest a central role for ERα-dependent modulation of high-level chromatin structure that permits other transcription factors to access their respective binding elements that were previously unavailable. We were also able to show, using a PR-B DBD mutant, that this localization requires DNA binding. Additionally, we used this model system to illustrate the cooperative loading phenomenon is specific for type I NRs, as PPARγ did not localize to the PRL array under dual ligand treatment. We cannot, however, exclude that members of other families of transcription factors could follow the same mechanism in this model, or that other NRs could use the same mechanism on a selected number of response elements in the whole genome. Studies on these scenarios are currently under way, but combined

with the work of Voss *et al*. is suggestive that type I NRs have this pioneering ability.

Our decision to further explore the mechanisms underlying the interplay between ERα and GR at the chromatin level is emphasized by the importance of both receptors in prognosis and treatment of breast cancer (40) and other pathologies including osteoporosis and inflammatory diseases (43). Moreover, GR is the only type I NR that is endogenously expressed in HeLa cells, thus facilitating mechanistic studies without the need of exogenous expression. Our development and application of custom, single-cell–based high-content analysis allowed us to quantify multiple mechanistic steps that are involved during or after *de novo* loading of endogenous GR to the PRL array. To address which domain of ERα was essential for recruitment of GR under dual ligand treatment, we used a series of well-characterized ERα mutants, and we found that helix-12 within the ligand-binding domain of ERα is required for GR loading onto the PRL array. Although other ERα domains may be playing a role as well (e.g. the DNA-binding domain), we observed a complete loss of GR loading with the helix-12 mutant, indicating a central role for this portion of the receptor. Moreover, ERβ, which has a different N-terminal domain from ERα, is still fully capable of recruiting GR. As helix-12 is the main structural feature that determines recruitment of co-regulatory factors, this observation raised the possibility that coactivators and their chromatin remodeling actions may be necessary requirement for GR recruitment to the array.

To test this hypothesis, we performed a small focused siRNA survey against selected transcriptional modulators. Our survey identified MED14, SRC-2 and SRC-3 as three co-regulators that are required for GR loading after dual agonist treatment, without effecting changes on ERα loading to the PRL array. Interestingly, a reduction in GR loading also occurred when we treated PRL-HeLa-ERα cells with E2 + RU486 after knockdown of MED14, suggesting a similar method of recruitment regardless of GR ligand (data not shown). This was an interesting observation, as MED14 and both SRC-2 and SRC-3 have been previously studied in the context of GR actions. MED14 has been shown to interact with the N-terminal AF-1 region of GR (44), leaving the C-terminal AF-2 region free to interact with other transcriptional regulators. In breast cancer cell lines, MED14 has also been shown to act as an ERα co-activator through helix-12 interaction (45), further implicating this component of the mediator complex as a scaffold for recruitment of additional factors. This is the first data to suggest a novel integrator role for mediator proteins to modulate recruitment to sites throughout the genome of different transcription factors under various hormonal stimuli.

From our initial RNAi survey, we also found that SRC-2 and SRC-3 are required for MED14 recruitment to the PRL array, but not vice versa, indicating that MED14 may be recruited as a second tier co-regulator to help recruit GR. Our study is also the first data on coactivators playing an important role in the assisted loading of transcription factors. It is also interesting to observe the compensatory effects of SRC-2 and SRC-3 on the ability of GR to load onto the PRL array. Previous reports have shown fewer compensatory (46,47) than non-compensatory (48–50) interactions between p160 family of coactivators. These suggest a greater role in complex transcriptional mechanisms for the p160 family members beyond transactivation and suggest modification of cross-talk in cancers that overexpress the coactivators.

The effect of the ERα/GR interplay was also queried at the level of transcriptional regulation, and we found that the presence of both GR and ERα at the PRL array causes a reduction in E2-mediated stimulation of gene transcription. However, this was not the only possible outcome, as, in MCF-7 cells, we observed both cooperation and antagonism on E2 regulated genes, as exemplified by the TFF1 and GREB1 mRNAs. The mechanism(s) underlying this phenomenon is not fully clear, and it is likely to be gene specific, with both issues calling for future investigations. We were also able to show cooperative interplay between ERα and GR in MCF-7 cells with a distinct transcriptional output at the GREB1 and TFF1 loci. The different styles of interplay in the enhancer regions of GREB1 and TFF1 demonstrate the need for additional studies examining how transcription factors are arrayed along the genome when multiple hormones are present, as clearly this is the more physiologically relevant context. Taken together, the results presented here highlight a mechanism by which GR (and/or other steroid NR receptors) can be recruited to previously inaccessible chromatin regions by a 'pioneering' role of ERα in chromatin remodeling and co-activator interaction that ultimately modulates ERα-regulated gene transcription. In particular, GR requires the combination of ERα, MED14 and SRC-2/-3 to be recruited. However, we and others have failed to observe a stable complex formation between ERα and GR using both co-immunoprecipitation and ChIP–reChIP experiments [data not shown and (15)], suggesting a dynamic relationship between transcription factors and co-regulators at enhancer elements. The observation of this interplay is an important step towards further dissection of steroid-mediated cross-talk between pathways that underlie transcriptional fine tuning to meet cellular requirements for homeostasis, or play aberrant roles during pathogenesis and disease development.

SUPPLEMENTARY DATA

Supplementary Data are available at NAR Online: Supplementary Figures 1–5.

ACKNOWLEDGEMENTS

The authors gratefully acknowledge the effort of M. G. Mancini and Z. D. Sharp for the development of the PRL-HeLa cell line, F. J. Ashcroft for creation of the GFP-ERα:PRL-HeLa cells, K. P. White (University of Chicago) for sharing GR ChIP-seq data sets and I. Mikic and T. J. Moran (Accelrys Inc., San Diego, CA,

USA) for development of the automated high-content analysis tools used in this study.

FUNDING

National Institute of Environmental Health Sciences Grand Opportunity award [1RC2ES018789]; Keck Foundation pre-doctoral fellowship and imaging/automation resource support from the John S. Dunn Gulf Coast for Chemical Genomics (P.J. Davies and M.A.M.); Dan L Duncan Baylor Cancer Center (K. Osborne); Center for Reproductive Biology (FJ Demayo), Keck Center NLM Training Program in Biomedical Informatics of the Gulf Coast Consortia National Library of Medicine [T15LM007093 to M.B]; National Institutes of Health K12 [DK0083014 to J.N.]; National Institute of Diabetes and Digestive and Kidney; the Diana Helis Henry Medical Research Foundation through its direct engagement in the continuous active conduct of medical research in conjunction with Baylor College of Medicine and the Cancer Program. Funding for open access charge: Helis Medical Research Foundations.

Conflict of interest statement. None declared.

REFERENCES

1. Horner-Glister,E., Maleki-Dizaji,M., Guerin,C.J., Johnson,S.M., Styles,J. and White,I.N. (2005) Influence of oestradiol and tamoxifen on oestrogen receptors-alpha and -beta protein degradation and non-genomic signalling pathways in uterine and breast carcinoma cells. *J. Mol. Endocrinol.*, **35**, 421–432.
2. Ogawa,S., Eng,V., Taylor,J., Lubahn,D.B., Korach,K.S. and Pfaff,D.W. (1998) Roles of estrogen receptor-alpha gene expression in reproduction-related behaviors in female mice. *Endocrinology*, **139**, 5070–5081.
3. Rudnik,V., Sanyal,A., Syed,F.A., Monroe,D.G., Spelsberg,T.C., Oursler,M.J. and Khosla,S. (2008) Loss of ERE binding activity by estrogen receptor-alpha alters basal and estrogen-stimulated bone-related gene expression by osteoblastic cells. *J. Cell. Biochem.*, **103**, 896–907.
4. Tobias,J.H., Steer,C.D., Vilarino-Guell,C. and Brown,M.A. (2007) Estrogen receptor alpha regulates area-adjusted bone mineral content in late pubertal girls. *J. Clin. Endocrinol. Metab.*, **92**, 641–647.
5. Pike,A.C. (2006) Lessons learnt from structural studies of the oestrogen receptor. *Best Pract. Res.*, **20**, 1–14.
6. Spears,M. and Bartlett,J. (2009) The potential role of estrogen receptors and the SRC family as targets for the treatment of breast cancer. *Expert Opin. Ther. Targets*, **13**, 665–674.
7. Lee,J.E., Kim,K., Sacchettini,J.C., Smith,C.V. and Safe,S. (2005) DRIP150 coactivation of estrogen receptor alpha in ZR-75 breast cancer cells is independent of LXXLL motifs. *J. Biol. Chem.*, **280**, 8819–8830.
8. Bernardo,G.M., Lozada,K.L., Miedler,J.D., Harburg,G., Hewitt,S.C., Mosley,J.D., Godwin,A.K., Korach,K.S., Visvader,J.E., Kaestner,K.H. *et al.* (2010) FOXA1 is an essential determinant of ERalpha expression and mammary ductal morphogenesis. *Development*, **137**, 2045–2054.
9. Giulianelli,S., Vaque,J.P., Soldati,R., Wargon,V., Vanzulli,S.I., Martins,R., Zeitlin,E., Molinolo,A.A., Helguero,L.A., Lamb,C.A. *et al.* (2012) Estrogen receptor alpha mediates progestin-induced mammary tumor growth by interacting with progesterone receptors at the cyclin D1/MYC promoters. *Cancer Res.*, **72**, 2416–2427.
10. Kong,S.L., Li,G., Loh,S.L., Sung,W.K. and Liu,E.T. (2011) Cellular reprogramming by the conjoint action of ERalpha, FOXA1, and GATA3 to a ligand-inducible growth state. *Mol. Syst. Biol.*, **7**, 526.
11. Stender,J.D., Stossi,F., Funk,C.C., Charn,T.H., Barnett,D.H. and Katzenellenbogen,B.S. (2011) The estrogen-regulated transcription factor PITX1 coordinates gene-specific regulation by estrogen receptor-alpha in breast cancer cells. *Mol. Endocrinol.*, **25**, 1699–1709.
12. Ross-Innes,C.S., Stark,R., Holmes,K.A., Schmidt,D., Spyrou,C., Russell,R., Massie,C.E., Vowler,S.L., Eldridge,M. and Carroll,J.S. (2010) Cooperative interaction between retinoic acid receptor-alpha and estrogen receptor in breast cancer. *Genes Dev.*, **24**, 171–182.
13. Hua,S., Kittler,R. and White,K.P. (2009) Genomic antagonism between retinoic acid and estrogen signaling in breast cancer. *Cell*, **137**, 1259–1271.
14. Pradhan,M., Bembinster,L.A., Baumgarten,S.C. and Frasor,J. (2010) Proinflammatory cytokines enhance estrogen-dependent expression of the multidrug transporter gene ABCG2 through estrogen receptor and NF{kappa}B cooperativity at adjacent response elements. *J. Biol. Chem.*, **285**, 31100–31106.
15. Voss,T.C., Schiltz,R.L., Sung,M.H., Yen,P.M., Stamatoyannopoulos,J.A., Biddie,S.C., Johnson,T.A., Miranda,T.B., John,S. and Hager,G.L. (2011) Dynamic exchange at regulatory elements during chromatin remodeling underlies assisted loading mechanism. *Cell*, **146**, 544–554.
16. Committee,N.R. (1999) A unified nomenclature system for the nuclear receptor superfamily. *Cell*, **97**, 161–163.
17. Riggio,M., Polo,M.L., Blaustein,M., Colman-Lerner,A., Luthy,I., Lanari,C. and Novaro,V. (2012) PI3K/AKT pathway regulates phosphorylation of steroid receptors, hormone independence and tumor differentiation in breast cancer. *Carcinogenesis*, **33**, 509–518.
18. Verma,M.K., Miki,Y. and Sasano,H. (2011) Sex steroid receptors in human lung diseases. *J. Steroid Biochem. Mol. Biol.*, **127**, 216–222.
19. Amazit,L., Pasini,L., Szafran,A.T., Berno,V., Wu,R.C., Mielke,M., Jones,E.D., Mancini,M.G., Hinojos,C.A., O'Malley,B.W. *et al.* (2007) Regulation of SRC-3 intercompartmental dynamics by estrogen receptor and phosphorylation. *Mol. Cell. Biol.*, **27**, 6913–6932.
20. Ashcroft,F.J., Newberg,J.Y., Jones,E.D., Mikic,I. and Mancini,M.A. (2011) High content imaging-based assay to classify estrogen receptor-alpha ligands based on defined mechanistic outcomes. *Gene*, **477**, 42–52.
21. Berno,V., Amazit,L., Hinojos,C., Zhong,J., Mancini,M.G., Sharp,Z.D. and Mancini,M.A. (2008) Activation of estrogen receptor-alpha by E2 or EGF induces temporally distinct patterns of large-scale chromatin modification and mRNA transcription. *PloS One*, **3**, e2286.
22. Sharp,Z.D., Mancini,M.G., Hinojos,C.A., Dai,F., Berno,V., Szafran,A.T., Smith,K.P., Lele,T.P., Ingber,D.E. and Mancini,M.A. (2006) Estrogen-receptor-alpha exchange and chromatin dynamics are ligand- and domain-dependent. *J. Cell Sci.*, **119**, 4101–4116.
23. Cao,Z.D., Barron,E.A. and Sharp,Z.D. (1988) Prolactin upstream factor I mediates cell-specific transcription. *Mol. Cell. Biol.*, **8**, 5432–5438.
24. Masood,S. (1992) Immunocytochemical localization of estrogen and progesterone receptors in imprint preparations of breast carcinomas. *Cancer*, **70**, 2109–2114.
25. Brugnatelli,S., Gattoni,E., Grasso,D., Rossetti,F., Perrone,T. and Danova,M. (2011) Single-dose palonosetron and dexamethasone in preventing nausea and vomiting induced by moderately emetogenic chemotherapy in breast and colorectal cancer patients. *Tumori*, **97**, 362–366.
26. Moutsatsou,P. and Papavassiliou,A.G. (2008) The glucocorticoid receptor signalling in breast cancer. *J. Cell. Mol. Med.*, **12**, 145–163.
27. Vaidya,J.S., Baldassarre,G., Thorat,M.A. and Massarut,S. (2010) Role of glucocorticoids in breast cancer. *Curr. Pharm. Des.*, **16**, 3593–3600.
28. de Hoon,M.J., Imoto,S., Nolan,J. and Miyano,S. (2004) Open source clustering software. *Bioinformatics*, **20**, 1453–1454.

29. Saldanha,A.J. (2004) Java Treeview—extensible visualization of microarray data. *Bioinformatics*, **20**, 3246–3248.
30. Garcia-Becerra,R., Berno,V., Ordaz-Rosado,D., Sharp,Z.D., Cooney,A.J., Mancini,M.A. and Larrea,F. (2010) Ligand-induced large-scale chromatin dynamics as a biosensor for the detection of estrogen receptor subtype selective ligands. *Gene*, **458**, 37–44.
31. Zwart,W., de Leeuw,R., Rondaij,M., Neefjes,J., Mancini,M.A. and Michalides,R. (2010) The hinge region of the human estrogen receptor determines functional synergy between AF-1 and AF-2 in the quantitative response to estradiol and tamoxifen. *J. Cell Sci.*, **123**, 1253–1261.
32. McGowan,E.M., Russell,A.J., Boonyaratanakornkit,V., Saunders,D.N., Lehrbach,G.M., Sergio,C.M., Musgrove,E.A., Edwards,D.P. and Sutherland,R.L. (2007) Progestins reinitiate cell cycle progression in antiestrogen-arrested breast cancer cells through the B-isoform of progesterone receptor. *Cancer Res.*, **67**, 8942–8951.
33. Cvoro,A., Yuan,C., Paruthiyil,S., Miller,O.H., Yamamoto,K.R. and Leitman,D.C. (2011) Cross talk between glucocorticoid and estrogen receptors occurs at a subset of proinflammatory genes. *J. Immunol.*, **186**, 4354–4360.
34. Gong,H., Jarzynka,M.J., Cole,T.J., Lee,J.H., Wada,T., Zhang,B., Gao,J., Song,W.C., DeFranco,D.B., Cheng,S.Y. *et al.* (2008) Glucocorticoids antagonize estrogens by glucocorticoid receptor-mediated activation of estrogen sulfotransferase. *Cancer Res.*, **68**, 7386–7393.
35. Watanabe,M., Noda,M. and Nakajin,S. (2007) Aromatase expression in a human osteoblastic cell line increases in response to prostaglandin E(2) in a dexamethasone-dependent fashion. *Steroids*, **72**, 686–692.
36. Lonard,D.M., Nawaz,Z., Smith,C.L. and O'Malley,B.W. (2000) The 26S proteasome is required for estrogen receptor-alpha and coactivator turnover and for efficient estrogen receptor-alpha transactivation. *Mol. Cell*, **5**, 939–948.
37. Madak-Erdogan,Z., Lupien,M., Stossi,F., Brown,M. and Katzenellenbogen,B.S. (2011) Genomic collaboration of estrogen receptor alpha and extracellular signal-regulated kinase 2 in regulating gene and proliferation programs. *Mol. Cell. Biol.*, **31**, 226–236.
38. Bookout,A.L., Jeong,Y., Downes,M., Yu,R.T., Evans,R.M. and Mangelsdorf,D.J. (2006) Anatomical profiling of nuclear receptor expression reveals a hierarchical transcriptional network. *Cell*, **126**, 789–799.
39. Buxant,F., Engohan-Aloghe,C. and Noel,J.C. (2010) Estrogen receptor, progesterone receptor, and glucocorticoid receptor expression in normal breast tissue, breast in situ carcinoma, and invasive breast cancer. *Appl. Immunohistochem. Mol. Morphol.*, **18**, 254–257.
40. Pan,D., Kocherginsky,M. and Conzen,S.D. (2011) Activation of the glucocorticoid receptor is associated with poor prognosis in estrogen receptor-negative breast cancer. *Cancer Res.*, **71**, 6360–6370.
41. Guo,C.M., Zhu,X.O., Ni,X.T., Yang,Z., Myatt,L. and Sun,K. (2009) Expression of progesterone receptor A form and its role in the interaction of progesterone with cortisol on cyclooxygenase-2 expression in amnionic fibroblasts. *J. Clin. Endocrinol. Metab.*, **94**, 5085–5092.
42. Leo,J.C., Guo,C., Woon,C.T., Aw,S.E. and Lin,V.C. (2004) Glucocorticoid and mineralocorticoid cross-talk with progesterone receptor to induce focal adhesion and growth inhibition in breast cancer cells. *Endocrinology*, **145**, 1314–1321.
43. Butler,J.S., Queally,J.M., Devitt,B.M., Murray,D.W., Doran,P.P. and O'Byrne,J.M. (2010) Silencing Dkk1 expression rescues dexamethasone-induced suppression of primary human osteoblast differentiation. *BMC Musculoskelet. Disord.*, **11**, 210.
44. Hittelman,A.B., Burakov,D., Iniguez-Lluhi,J.A., Freedman,L.P. and Garabedian,M.J. (1999) Differential regulation of glucocorticoid receptor transcriptional activation via AF-1-associated proteins. *EMBO J.*, **18**, 5380–5388.
45. Lee,J. and Safe,S. (2007) Coactivation of estrogen receptor alpha (ER alpha)/Sp1 by vitamin D receptor interacting protein 150 (DRIP150). *Arch. Biochem. Biophys.*, **461**, 200–210.
46. Tien,J.C., Zhou,S. and Xu,J. (2009) The role of SRC-1 in murine prostate cancinogenesis is nonessential due to a possible compensation of SRC-3/AIB1 overexpression. *Int. J. Biol. Sci.*, **5**, 256–264.
47. Xu,J. and Li,Q. (2003) Review of the *in vivo* functions of the p160 steroid receptor coactivator family. *Mol. Endocrinol.*, **17**, 1681–1692.
48. Grenier,J., Trousson,A., Chauchereau,A., Amazit,L., Lamirand,A., Leclerc,P., Guiochon-Mantel,A., Schumacher,M. and Massaad,C. (2004) Selective recruitment of p160 coactivators on glucocorticoid-regulated promoters in Schwann cells. *Mol. Endocrinol.*, **18**, 2866–2879.
49. Hartig,S.M., He,B., Long,W., Buehrer,B.M. and Mancini,M.A. (2011) Homeostatic levels of SRC-2 and SRC-3 promote early human adipogenesis. *J. Cell Biol.*, **192**, 55–67.
50. Wu,H.Y., Hamamori,Y., Xu,J., Chang,S.C., Saluna,T., Chang,M.F., O'Malley,B.W. and Kedes,L. (2005) Nuclear hormone receptor coregulator GRIP1 suppresses, whereas SRC1A and p/CIP coactivate, by domain-specific binding of MyoD. *J. Biol. Chem.*, **280**, 3129–3137.